

Testing an Impedance Non-destructive Method to Evaluate Steel-Fiber Concrete Samples

Tereza Komarkova¹, Pavel Fiala², Miloslav Steinbauer³, Zdenek Roubal³

¹ Department of Building and Testing, Faculty of Civil Engineering, BUT, Veveří 95, 602 00, Brno, Czech Republic, tereza.komarkova@vutbr.cz

² SIX Centre, FEEC, BUT, Technická 3082/12, 616 00, Brno, FEEC, BUT, Technická 3082/12, 616 00 Brno; Czech Republic

³ Department of Theoretical and Experimental Electrical Engineering, FEEC, BUT, Technická 3082/12, 616 00, Brno; Czech Republic

Steel-fiber reinforced concrete is a composite material characterized by outstanding tensile properties and resistance to the development of cracks. The concrete, however, exhibits such characteristics only on the condition that the steel fibers in the final, hardened composite have been distributed evenly. The current methods to evaluate the distribution and concentration of a fiber composite are either destructive or exhibit a limited capability of evaluating the concentration and orientation of the fibers. In this context, the paper discusses tests related to the evaluation of the density and orientation of fibers in a composite material. Compared to the approaches used to date, the proposed technique is based on the evaluation of the electrical impedance Z in the band close to the resonance of the sensor-sample configuration. Using analytically expressed equations, we can evaluate the monitored part of the composite and its density at various depths of the tested sample. The method employs test blocks of composites, utilizing the resonance of the measuring device and the measured sample set; the desired state occurs within the interval of between $f=3$ kHz and 400 kHz.

Keywords: Steel-fiber; concrete; non-destructive testing; electromagnetic field; electric impedance.

1. INTRODUCTION

The last decades have witnessed major development of fiber-reinforced concrete, a material formed through the addition of a metal reinforcement (filler), but also the general rise of interest in composite materials and related non-destructive testing methods [1]-[7].

In order for a material to exhibit the required mechanical and thermal properties, it is necessary to ensure the related macroscopic properties, such as the homogeneous and isotropic distribution of the components, and thus also the resulting parameters. This phase depends on selecting a suitable technology to prepare and manufacture the given material. Intensive attention is thus paid to methods and principles that enable us to evaluate non-destructively the concentration of the components of a composite, fillers in particular; by extension, these approaches are also employed to assess the orientation of individual elements in a concrete filler [6], [8]-[10]. An interesting tool consists of techniques and devices to evaluate the concentration of fibrous particles, or steel fibers, in both fresh and solidified concrete; in this case, however, the orientation of the fibers can be assessed only with considerable difficulty.

The presently used techniques exploit the common evaluation of the electrical impedance Z of the tested sample [4], [5], and they employ dedicated experiments to derive the relationship between changes of the module of the electrical impedance Z and orientation of the steel fibers. Generally, researchers point out the relationship between the impedance magnitude and the concentration of the fibers.

Our experiments have shown that, utilizing the electric and ferromagnetic properties of steel fibers as the composite filler component in reinforced concrete, it is possible to monitor the concentration and distribution of the fibers in a non-destructive manner [1]. Further, the use of a suitable measurement methodology and the frequency band close to the resonance of the sensor-sample configuration facilitates more accurate derivation and evaluation of the composition of the monitored composite component, namely, the steel fibers [1], [13].

2. THE IMPEDANCE MEASURING METHOD AND THE NEAR-RESONANCE STATE

The non-destructive methods presented to date, such as those discussed in papers [11]-[12], exploit the properties of the electromagnetic (EMG) field to monitor the distribution

of fibers in the tested composite. To evaluate the properties of the composite components, the actual principle employs the electric impedance \hat{Z} in the region of the monitored sample; we can then write

$$\hat{Z} = \frac{|\hat{E}|}{|\hat{H}|}, \quad (1)$$

where \hat{Z} denotes the complex impedance of the harmonic behavior of the electric and magnetic field components, \hat{E} is the complex vector of the electric field intensity, and \hat{H} denotes the complex vector of the magnetic field intensity. The details of the fields and other aspects are shown in, for example, Fig.1. The frequency f of the impedance meter's excitation signal (Fig.1.) is progressively set such that the resonance quality factor Q_h could assume the values

$$Q_{0.5} = \frac{1}{2} Q_{max}, \quad Q_{sq2} = \frac{1}{\sqrt{2}} Q_{max}, \quad Q_{sq3} = \frac{1}{\sqrt{3}} Q_{max} \quad (2)$$

In the experimental setting, the values proved to be beneficial for the final evaluation of the location with non-uniform distribution of the composite material components. To evaluate the mass density of the monitored composite material component, the electric power specific density (the Poynting vector) is assessed; this vector is then written as

$$\hat{\Pi} = \hat{E} \times \hat{H}, \quad (3)$$

where the symbol \times denotes the vector product.

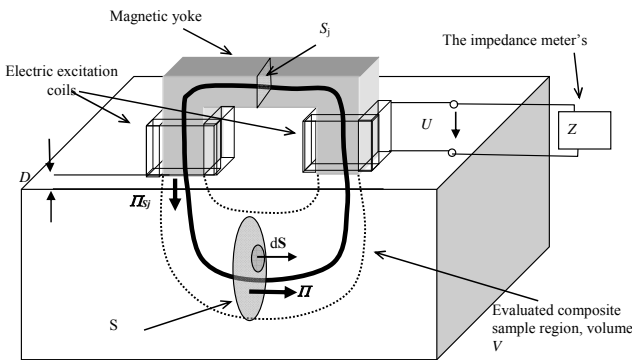


Fig.1. A scheme of the impedance-based NDT method: the evaluation of the tested sample parameters.

The dissipated electrical power P generated in the monitored composite material component is bound to the surface density of the active power $\hat{\Pi}$ from the above expression (3), and this dissipated power is formulated within

$$P = \int_{S_j} \hat{\Pi}_{S_j} \cdot dS, \quad (4)$$

where P is the dissipated electrical power in the region having the volume V in the measured portion of the composite material, $\hat{\Pi}_{S_j}$ denotes the power flux surface density in the area of the shaping yoke at the distance D from the surface of the composite material, dS is the vector of the element of the cross section area of the measured part of the composite material sample, S_j represents the section through the magnetic yoke, and S is the cross section of the area of the monitored material sample (Fig.1.).

In relation to the preset resonant frequency f_r of the entire setup comprising a detection and measuring device and an electric coil wound on the arms of a ferromagnetic yoke, we have – for the complex impedance \hat{Z} in the exponential form – the formula

$$\hat{Z}_0|_{f_r} = \frac{|\hat{E}|}{|\hat{H}|} \angle \varphi_0, \varphi_0 \cong 0. \quad (5)$$

For the component form, the complex impedance is written as

$$\hat{Z}_0|_{f_r} = Z_{0,Re} + jZ_{0,Im}, \forall f = f_r, \text{ holds } Z_{0,Im} \cong 0, \quad (6)$$

where $Z_{0,Re}$, $Z_{0,Im}$ are the real and imaginary components of the complex impedance \hat{Z} . Based on such measured data, it is then easy to evaluate the magnitude of the dissipated power (3), which corresponds to the mass density of the monitored composite material component

$$P = \text{Re} \left\{ \frac{U^2}{\hat{Z}_0} \right\}, \quad (7)$$

where U is the effective value (RMS) of the electric voltage on the terminals of the excitation coils in Fig.1.

The change of resonance for the initial preset frequency f_r of the detection and measuring device and the connected electric coil will occur if the position of the ferromagnetic yoke is altered such that, in the monitored volume V of the tested composite material sample, we can observe a variation of the mass density ρ or the orientation of the needle-like formations of the monitored composite material components.

Using the above-expressed relationships between the mass density of the composite material component and the electromagnetic field, (3) to (7), it is possible to evaluate the parameters of the desired properties of the composite material samples according to the function g :

$$U^2 = g(J^2, \gamma_{ef}^2, S(f)), \quad (8)$$

where J is the current density in the volume V , and γ_{ef} denotes the equivalent specific electrical conductivity in the volume V , Fig.1.

3. EVALUATING THE TESTS OF BLOCKS AND PARAMETERS

The proposed methodology tests [13] were performed in laboratory conditions, Fig.2. The actual testing of the composite material sample (with the applied needle-like filler components, Fig.3., Fig.4., and Fig.5.) for the selected type and version of the magnetic yoke within the given frequency range is shown in Fig.6.

To enable the testing and evaluation of the specific density of the monitored parts of the composite ρ (Fig.5.) in the block of the sample (Fig.3.), we assessed the losses dP [W] in the measured area as having volume V . In the sample P4 from Fig.3., given the frequency of $f_r=328.630$ kHz, we determined the losses of $dP_{co}=39.1 \mu\text{W}$ and $dP_{fi}=37.0$ mW on the fine and coarse sides ($\Delta x_{fi}<0.2$ mm and $\Delta x_{co}\cong 10$ mm, respectively). The reference structures lacking metal elements of the composite, $dP_{fant} = 0.349$ mW, and the composite distribution characteristics were analyzed differently (Fig.7., Fig.8., and Fig.11.). A similar test was performed for the same sample at the frequency of $f_r=146.000$ kHz, again involving both the fine ($\Delta x_{fi}<0.2$ mm) and the coarse ($\Delta x_{co}\cong 10$ mm,) sides; the relevant evaluated losses corresponded to $dP_{co}=30.6$ mW and $dP_{fi}=36.6$ mW. The reference structures lacking metal elements of the composite exhibited the value of $dP_{fant} = 22.8$ mW (Fig.9., Fig.10., and Fig.12.).



Fig.2. The measuring test system and recording device (NDT) to evaluate the impedance module/phase of the monitored component at the DTEEE laboratories.

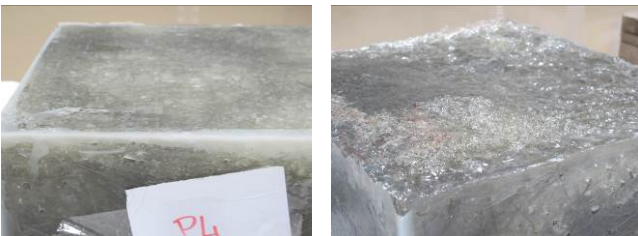


Fig.3. The composite material sample (P4) tested at the DTEEE laboratories; the dimensions are 300x300x140 mm.



Fig.4. The compact NDT measurement and recording device to evaluate the impedance module/phase of the monitored component of the composite material sample. The apparatus operates as a semi-automatic monitoring system.

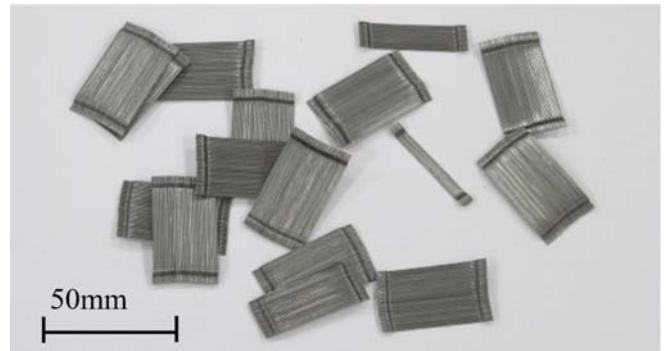


Fig.5. Selected metal elements of the monitored component of the composite material sample.

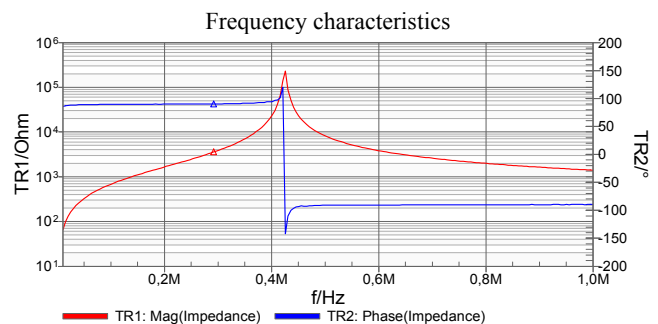


Fig.6. The frequency characteristics of the magnetic yoke: the resonant frequency of $f_r=425.000$ kHz.

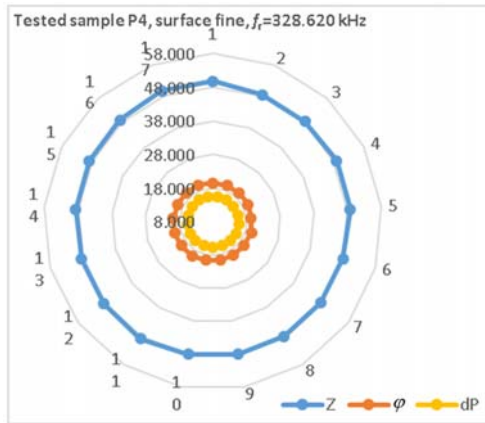


Fig.7. The measurement and evaluation of the impedance module/phase of the monitored component P4, impedance module Z , $f_r=328.630$ kHz: the fine surface, coarseness rate of $\Delta x_{fi} < 0.2$ mm.

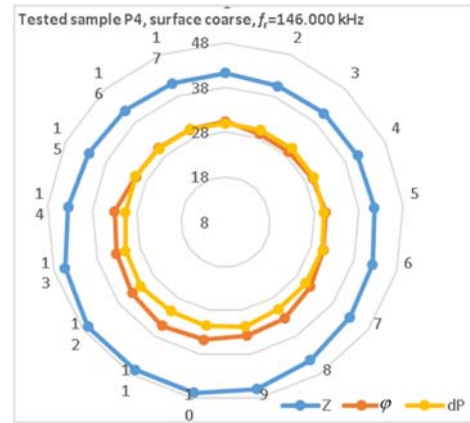


Fig.10. The measurement and evaluation of the impedance module/phase of the monitored component P4, impedance module Z , $f_r=146.000$ kHz: the coarse surface, coarseness rate of $\Delta x_{co} \cong 10$ mm.

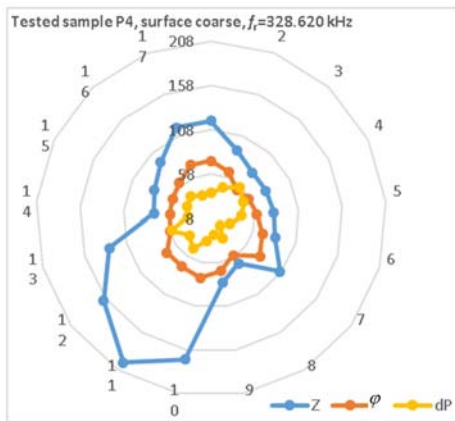


Fig.8. The measurement and evaluation of the impedance module/phase of the monitored component P4, impedance module Z , $f_r=328.630$ kHz: the coarse surface, coarseness rate of $\Delta x_{co} \cong 10$ mm.

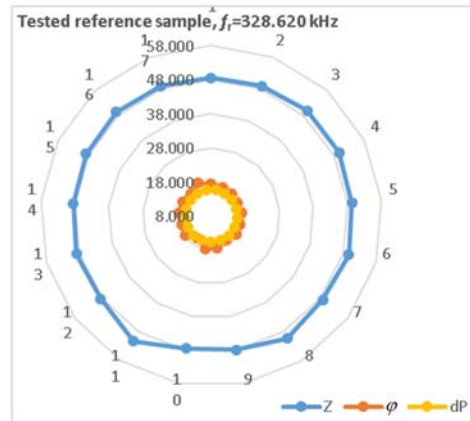


Fig.11. The measurement and evaluation of the impedance module/phase of the monitored component without the metal element, impedance module Z , $f_r=328.620$ kHz.

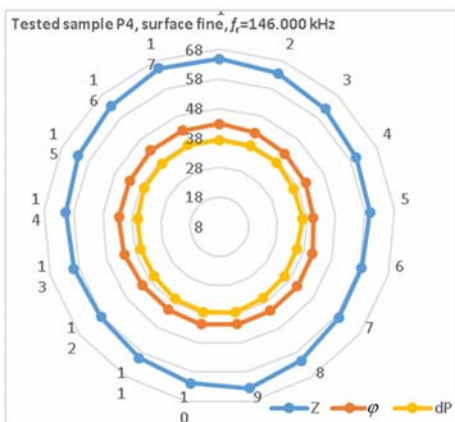


Fig.9. The measurement and evaluation of the impedance module/phase of the monitored component P4, impedance module Z , $f_r=146.000$ kHz: the fine surface, coarseness rate of $\Delta x_{fi} < 0.2$ mm.

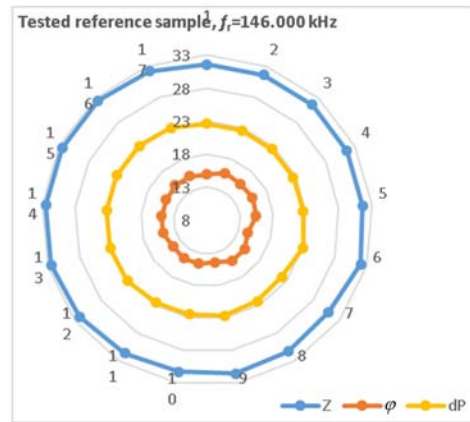


Fig.12. The measurement and evaluation of the impedance module/phase of the monitored component without the metal element, impedance module Z , $f_r=146.000$ kHz.

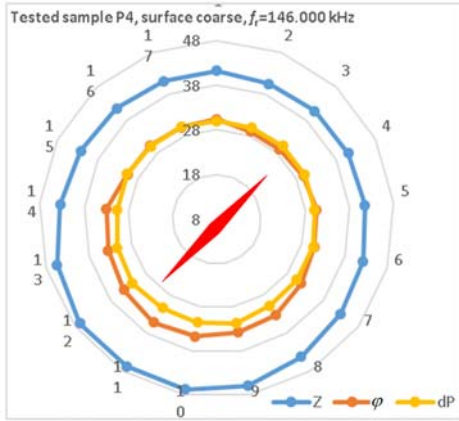


Fig.13. The measurement and evaluation of the impedance module/phase; a part of the composite orientation (red) in the monitored component P4, impedance module Z , $f_i=146.000$ kHz: the coarse surface, coarseness rate of $\Delta x_{co} \approx 10$ mm.

4. RESULTS

The results obtained from the blocks with the tested and evaluated distribution (homogeneity) of the composite material components, Fig.5., were analyzed for the frequencies of $f_{i1}=3.450$ kHz, $f_{i2}=21.900$ kHz, $f_{i3}=50.120$ kHz, $f_{i4}=146.000$ kHz, and $f_{i5}=328.630$ kHz. These frequencies had been preset to facilitate the evaluation of the dissipated power dP and, subsequently, the volumetric mass density ρ of the monitored metal elements. Using a simple test, we determined the volumes V_i , $i=1, \dots, 5$ actively influenced by the magnetic field generated by the magnetic yoke (Fig.1.). In evaluating the volumetric mass density ρ , it is possible to further utilize the already assessed volumes $V_5 \approx 75$ cm³, $V_4 \approx 375$ cm³, $V_3 \approx 600$ cm³, $V_2 \approx 900$ cm³, and $V_1 \approx 1125$ cm³. The coefficient k_V is then instrumental towards establishing the measured density of the metal composite ρ_{sam} ; in this context, we assume steel exhibiting the specific electric conductivity and volumetric mass density of $\gamma=9.93$ MS/m and ρ_{Fe} , respectively.

The resulting volumetric mass density of the tested sample corresponds to

$$\rho_{sam} = \rho_{Fe} k_V \cdot \quad (9)$$

We then employ the above formula (7) to express the content coefficient of the monitored composite component, from which the volumetric mass density ρ is enumerated.

The density coefficient of the monitored composite component corresponds to

$$k_V = \frac{4\pi(dP - dP_{fant})}{U^2} Z_{v,Re}, \quad (10)$$

where dP_{fant} is the previously measured and evaluated magnitude of the dissipated power of the reference structure without the monitored composite. For the sample P4 at the depth of down to 10 mm from the surface, we then have $\rho_{P4,f,10mm} = 87.2$ kg/m³ from the fine side and $\rho_{P4,co,10mm}$

= -135 kg/m³ from the coarse side. A similar analysis can be performed for the depth of 50 mm, with $\rho_{P4,f,50mm} = 61.4$ kg/m³ and $\rho_{P4,co,50mm} = 27.6$ kg/m³ from the fine and coarse sides, respectively.

5. DISCUSSION

The measurement results presented within the previous chapter can be characterized and commented upon as follows:

1. It is invariably advisable to consider the analyses from the perspective of the reference sample, namely, the sample where the composite component has been eliminated (as characterized above in the form of the parameter dP_{fant}).

2. Fig.7. to Fig.12. can be used to interpret the inhomogeneities in the distribution of the monitored composite component, and these are then evaluable from the components of the modulus of the impedance Z , phase φ , and dissipated power dP in the graphical embodiment of the radial interpretation of the quantities.

3. Analyses where the properties of the tested sample are assessed at different depths have to assume the parameters of the electromagnetic field. As already indicated within related sections of the text, the low-quality surface finishes (namely, the highly coarse ones) exhibit – considering analyses down to 10 mm – a major difference between the evaluated density rates in the monitored composite component; this effect becomes obvious if we compare the parameters and graphs from Fig.7., Fig.8. and active losses $dP_{co} = 39.1$ μ W, $dP_{fi} = 37.0$ mW. The data differ to such an extent that, considering the technology applied to produce the sample, they can be regarded as inadequate values. The claim is verifiable via performing a measurement cycle in greater depths, for example, down to 50 mm below the surface; the data obtained for the depths of 10 mm and 50 mm differ fundamentally. An identical reference sample is characterized by the losses of $dP_{co} = 30.6$ mW, $dP_{fi} = 36.6$ mW, namely, values corresponding to the applied technology for fabricating the tested sample.

4. The evaluation of the density of the metal elements, namely, the monitored composite component, is derived from the dissipated power dP in the assumed space to be observed having volume V . In an inappropriately preset measurement cycle (or one where the low quality sample surface finish exhibits high roughness), including the influence of the remaining composite components in the form of dissipated power, dP_{fant} , will result in erroneous data on the volumetric mass density of the material of the component. Within our exemplary measurement, the information corresponding to such a condition is $\rho_{P4,co,10mm} = -135$ kg/m³, a value that points to inappropriate setting of the measurement and analysis of the sample.

6. CONCLUSION

We designed and tested a novel methodology using impedance in the complex form to facilitate NDT-based

measurement and evaluation of composite material components.

Test samples of composite materials with needle-like formations applied as the reinforcement were experimentally measured in laboratory conditions; in this context, we proved the basic functional principles of the designed NDT methodology for evaluating the distribution, density, and orientation of ferromagnetic/non-ferromagnetic conductive fibers in a composite material.

This novel metrological approach towards the NDT of composite materials exploits impedance analysis; the selected resonant frequency enables us to evaluate the quality of the examined composite at different depths below the surface of the given block sample.

The single-purpose devices designed and tested to support the NDT methodology exhibited sufficient sensitivity to evaluate the monitored components.

The outcomes of the measurement and evaluation of the fibers' directions and density are presented in chapters 3 and 4 above. Without major corrections, we evaluated the density (mass) of the steel fibers, which exhibited specific distribution density values at particular subsurface depths. The procedure proved to be valid and advantageous for use at frequencies within the band close to the resonance of the monitored region of the material.

Further research in the presented context will focus on verifying the accuracy of the volumetric mass density evaluation in the monitored composite material components.

ACKNOWLEDGEMENT

The research described herein was funded by the National Sustainability Program under grant No. LO1401. For the actual analyses and experiments, the infrastructure of the SIX Center was used.

REFERENCES

- [1] Fiala, P., Friedl, M., Hobst, L., Komarkova, T. (2014). *Method of evaluating distribution, density and orientation of ferromagnetic electrically conducting fibers within composite material and detection device for making the same*. Czech Patent Application PV2014-742.
- [2] Wang, W., Dai, Y., Zhang, C., Gao, X., Zhao, M. (2016). Micromechanical modeling of fiber-reinforced composites with statistically equivalent random fiber distribution. *Materials*, 9 (8), E624.
- [3] Giasin, K., Ayvar-Soberanis, S. (2016). Evaluation of workpiece temperature during drilling of GLARE fiber metal laminates using infrared techniques: Effect of cutting parameters, fiber orientation and spray mist application. *Materials*, 9 (8), E622.
- [4] Zou, S., Wan, Z., Lu, L., Tang, Y. (2016). Experimental study on tensile properties of a novel porous metal fiber/powder sintered composite sheet. *Materials*, 9 (9), E712.
- [5] Mizukami, K., Mizutani, Y., Kimura, K., Sato, A., Todoroki, A., Suzuki, Y. (2016). Detection of in-plane fiber waviness in cross-ply CFRP laminates using layer selectable eddy current method. *Composites Part A: Applied Science and Manufacturing*, 82, 108-118.
- [6] Zheng, K., Chang, Y.S., Wang, K.H., Yao, Y. (2016). Thermographic clustering analysis for defect detection in CFRP structures. *Polymer Testing*, 49, 73-81.
- [7] Santoro, S., Drioli, E., Figoli, A. (2016). Development of novel ECTFE coated PP composite hollow-fiber membranes. *Coating*, 6 (3), 40.
- [8] Martinie, L., Roussel, N. (2011). Simple tools for fiber orientation prediction in industrial practice. *Cement and Concrete Research*, 41 (10), 993-1000.
- [9] Shah, A.A., Ribakov, Y. (2011). Recent trends in steel fibered high-strength concrete. *Materials and Design*, 32 (8-9), 4122-4151.
- [10] Ozyurt, N., Mason, T.O., Shah, S.P. (2006). Non-destructive monitoring of fiber orientation using AC-IS: An industrial-scale application. *Cement and Concrete Research*, 36 (9), 1653-1660.
- [11] Szymanik, B., Frankowski, P.K., Chady, T., Azariah, C.R., Szczecin, J.C. (2015). Detection and inspection of steel bars in reinforced concrete structures using active infrared thermography with microwave excitation and eddy current. *Sensors*, 16 (2), 234.
- [12] Hobst, L., Bilek, P., Vodička, J., Vala, J. (2014). Measurement of set fibre-concrete homogeneity in finished steel fibre-concrete structure of segmental tunnel lining. *Advanced Materials Research*, 1106, 41-44.
- [13] Fiala, P., Friedl, M., Hobst, L., Komarkova, T. (2015). *A method and a detection device for evaluating the distribution, density and orientation of ferromagnetic, electrically conductive fibres in a composite material*. International Patent Application PCT/CZ2015/000132, publ. no. WO 2016070859 A1.

Received November 15, 2017.

Accepted February 20, 2018.